Active Management of Low-Voltage Networks for Mitigating Overvoltages due to Photovoltaic Units

Frédéric Olivier, *Student Member, IEEE,* Petros Aristidou, *Student Member, IEEE,*
Damien Ernst, *Member, IEEE,* and Thierry Van Cutsem, *Fellow, IEEE*

***Abstract*—In this paper, the overvoltage problems that might arise from the integration of photovoltaic panels into low-voltage distribution networks is addressed. A distributed scheme is proposed that adjusts the reactive and active power output of inverters to prevent or alleviate such problems. The proposed scheme is model-free and makes use of limited communication between the controllers, in the form of a distress signal, only during emergency conditions. It prioritizes the use of reactive power, while active power curtailment is performed only as a last resort. The behavior of the scheme is studied using dynamic simulations on a single low-voltage feeder and on a larger network composed of 14 low-voltage feeders. Its performance is compared to a centralized scheme based on the solution of an Optimal Power Flow problem, whose objective function is to minimize the active power curtailment. The proposed scheme successfully mitigates overvoltage situations due to high photovoltaic penetration and performs almost as well as the Optimal Power Flow based solution with significantly less information and communication requirements.**

***Index Terms*—low-voltage photovoltaic systems, active distribution network management, voltage control**

I. Introduction

During the last decades, the cost of PhotoVoltaic (PV) panels has been continuously decreasing. It is estimated that with each doubling of installed capacity, the cost of PV installations decreases by 20% [1]–[3]. This leads to the rapid growth of PV installations in Low-Voltage (LV) Distribution Networks (DNs).

However, the presence of power generation inside LV DNs changes the voltage profile of the feeders [4]. If the total installed PV power is larger than the feeder hosting capacity, i.e. the maximum amount of PV that can be accommodated, network security cannot be guaranteed [5]. Specifically, when the production of a feeder surpasses its consumption, a reverse power flow occurs which leads to overvoltages and might cause problems to the coordination of protective devices and disconnection of equipment for security reasons [6]. This important problem is studied in this paper.

The classical approach for addressing this issue is to rely on hefty investments to upgrade and reinforce the networks. However, many companies and researchers are looking at better ways to use existing equipment by developing and designing flexible and inexpensive control schemes to limit those investments and increase the hosting capacity of the networks [7].

These schemes, referred to under the term of Active Network Management, usually control the DNs' power generation, consumption or storage to prevent or mitigate overvoltage problems.

A. Literature review

Some of the schemes proposed in the literature can be classified as centralized: the control actions are computed by a common entity responsible for gathering information about the network, processing them according to some optimization objectives and constraints, and sending the set-points back to the actuators. In such schemes, the computation of the control actions often relies on an Optimal Power Flow (OPF) formulation of the problem and requires an extended communication infrastructure as well as a network model.

In Ref. [8], an OPF formulation with the objective to minimize the market value of the curtailed energy of embedded wind generation is proposed. Other objectives include minimizing the voltage profile deviation from a reference [9], the transformer tap changer switching [10], or the network losses [11], [12]. Ref. [13] studies a combination of those objectives. In Ref. [14], a sequential decision making problem under uncertainty is formulated where the Distribution System Operator has the choice to reserve the availability of flexible demand and, in the subsequent steps, to curtail generation and vary flexible loads. The aforementioned centralized schemes are defined and simulated in the framework of Medium Voltage (MV) networks.

Following, a second category of schemes are distributed: the units are controlled in a distributed way with no centralized control entity. The distributed controllers often use local information to adjust each unit individually.

Concerning the overvoltage problems considered in this work, it has been proposed to change the reactive power production [15], [16] or power factor [17], [18] of PV units, as a function of their terminal voltage. Alternatively, the use of active power curtailment [19] or storage of the excess energy in batteries [20] have been suggested.

In Refs. [21] and [22], it is suggested to compensate the voltage variations caused by changes in the PV generation with the use of reactive power and appropriate voltage sensitivity models. An adaptive control of reactive power production is used in [23], providing a compromise between the operation of the PV unit at unitary power factor and voltage control.

Frédéric Olivier, Petros Aristidou and Damien Ernst are with the Department of Electrical Engineering and Computer Science, University of Liège, Belgium, e-mail: {frederic.olivier,p.aristidou,dernst}@ulg.ac.be

Thierry Van Cutsem is with the Fund for Scientific Research (FNRS) at the Department of Electrical Engineering and Computer Science, University of Liège, Belgium, e-mail: t.vancutsem@ulg.ac.be

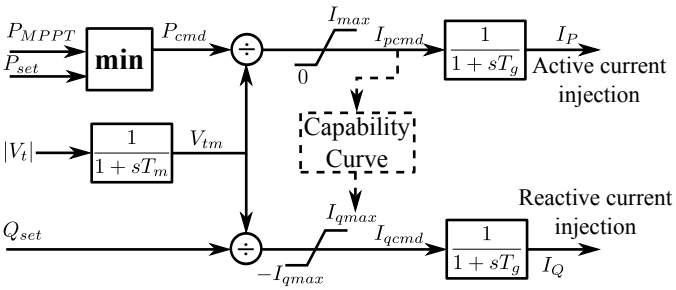

Figure 1. PV dynamic model

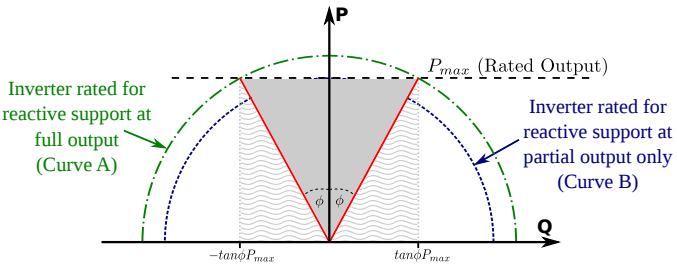

Figure 2. PV capability curve under constant voltage

Refs. [24] and [25] explicitly use communication to make a group of PV units converge to a percentage of the available power and regulate a critical bus. In Ref. [26], the voltage of the MV network is regulated thanks to a two-way communication between the transformer tap changer, the capacitor banks and the distributed generation units.

In Ref. [27] the benefits of using an inverter with STATCOM-like capabilities to regulate voltage variations caused by other sources or loads during night are presented. Finally, a comparison between an OPF-based centralized scheme and the distributed scheme of Ref. [28] is performed in [29].

A third category of control schemes, consisting of a combination of centralized and distributed schemes, are referred to as decentralized. More specifically, they are composed of local controllers and a centralized entity which computes the control law to be sent to them, so some communication is always needed. Once the control law is received, inverters do not need other control orders from the central entity to operate. Refs. [30]–[33] propose a decentralized control scheme of the reactive power to control the voltage and/or minimize system losses. Based on voltage sensitivity analysis, the authors of [34] suggest a control scheme to achieve the same goals, while [35] aims at minimizing the losses inside a microgrid.

B. Contributions of this paper

In this paper, a *distributed* control scheme that changes the active and reactive power injected by PV units in LV DNs is proposed. The objective of the control algorithm is to mitigate overvoltage problems by directing PV units to consume reactive power and, if necessary, to curtail active power generation. The distributed controllers are implemented on the PV inverters with five modes of operation.

First, if there are no overvoltage problems in the LV feeder, the controllers act preventively adjusting the PV units' reactive power to avert their occurrence while performing Maximum Power Point Tracking (MPPT) for active power. In this mode of operation, only local measurements are used and no communication among the controllers is needed. Second, if overvoltage problems occur, the controllers make use of limited communication for coordinating their reactive power consumption, within each DN LV feeder. Third, if the overvoltage persists even after all PV units have utilized their maximum reactive capabilities, the controllers switch to active power curtailment. Finally, the fourth and fifth modes of operation restore active and reactive power production to normal operation. The proposed scheme is model-free, as the model and parameters of the DN are not required by the controllers.

The behavior of the proposed control scheme is studied first on a single LV feeder and then on a larger network composed of 14 low-voltage feeders. Following, it is compared to a centralized OPF-based scheme applied to the same systems. Their performance is assessed based on their ability to alleviate the overvoltage problems and the amount of active power curtailed to achieve this. Both control schemes manage to ensure the security of the system. However, the OPF-based does this with a little less curtailed active power.

On the other hand, the main contribution of the proposed scheme is that it does not require a network model or remote measurements, thus making it easy to deploy. Moreover, the use of communication is limited to a distress signal that can be easily implemented with the use of Power-Line Communication (PLC) [36]. This technology has been exploited for several decades to provide low-cost remote switching capabilities to utilities; one such example is the day/night tariff signal used in some countries [37].

Additionally, it does not require a centralized entity to collect measurements, compute set-points and dispatch the PV units. Thus, it is more robust to component failures. Finally, when active power curtailment is required to secure the system, the proposed scheme is designed to proportionally share the burden among all the PV units in the problematic feeder.

The paper is organized as follows. In Section II the dynamic model of the PV units is presented. In Section III the proposed distributed control is detailed. Section IV introduces the centralized OPF-based scheme used for performance evaluation. The test systems and simulation results are reported in Section V. Finally, conclusions and future work are presented in Section VI.

II. PV UNIT DYNAMIC MODEL

The dynamic PV unit model selected for this study is detailed in Fig. 1. The closed-loop voltage regulator and the DC dynamics have been neglected for simplicity [38]. The model reflects active power priority with the active current command (I_{pcmd}) limited by the rating of the inverter (I_{max}). P_{set} and Q_{set} are the active and reactive power set-points computed by the controller detailed in the next section. When $P_{set} \geq P_{MPP}$, the unit operates in MPPT mode. T_g ($\sim$20 ms) and T_m ($\sim$50 ms) are the inverter current and voltage measurement time constants, respectively. Finally, the limits

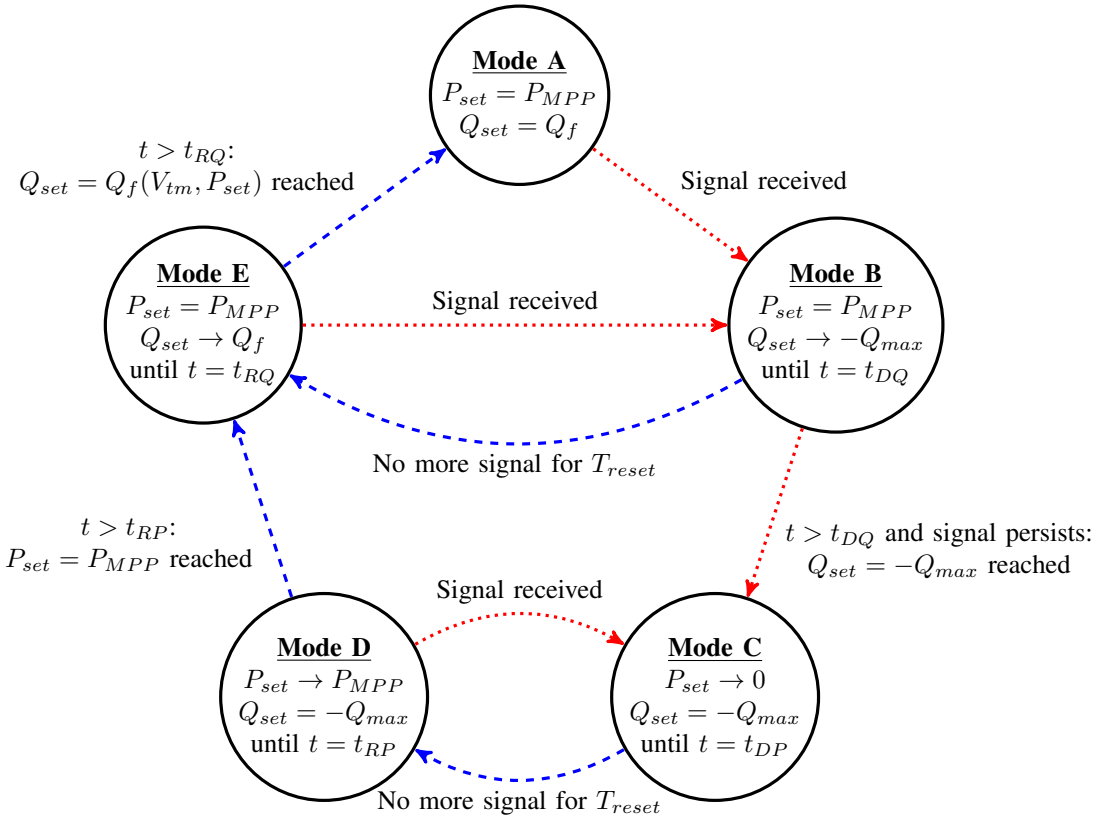

Figure 3. State transition diagram of the distributed control scheme. The red dotted lines are the emergency control transitions while blue dashed lines are the restoring ones. t_{DQ} (resp. t_{DP}) is the time needed in Mode B (resp. Mode C) to use all available reactive (resp. active) controls. T_{reset} is the elapsed time without emergency signal for the controller to start restoring active/reactive power. t_{RP} (resp. t_{RQ}) is the time needed in Mode D (resp. Mode E) to restore active (resp. reactive) power to the set-point values of Mode A. P_{set} and Q_{set} are the active and reactive power set-points of the controller. P_{MPP} is the maximum available active power of the PV module and depends on the solar irradiation. Q_{max} is the maximum available reactive power; it varies according to the capability curve (e.g. Fig. 2) as a function of the active power output.

on the reactive current command (I_{qcmd}) are calculated from the unit's reactive power capability curve using I_{pcmd}.

The capability curves of PV inverters are usually defined by the standards and grid codes of the country. In the recent years, numerous international and national standards and guidelines have been published, by different types of organizations (e.g. CENELEC, VDE, CEI), to introduce the new concept that LV active users have to provide some sort of ancillary services to the grid by adjusting their reactive power exchanged [39]–[41].

For example, the German standard VDE-AR-N 4105 [42] dictates that all DGs connected to LV grids should apply a Power Factor (PF) adjustment in order to contribute to the network voltage regulation according to their nominal power. For units smaller than 3.68 kVA a PF between $0.95_{leading}$ to $0.95_{lagging}$ is necessary according to DIN EN 50438 [40], for units between 3.68 and 13.8 kVA a characteristic curve provided by the network operator within $PF = 0.95_{leading}$ to $PF = 0.95_{lagging}$ and for larger units a characteristic curve provided by the network operator within $PF = 0.90_{leading}$ to $PF = 0.90_{lagging}$.

The latter PF ranges are visualized by the triangular shaded area in Fig. 2 and the reactive current limit can be computed as:

$$I_{qmax} = I_{pcmd} \tan\left(\cos^{-1} PF_{\min}\right) \quad (1)$$

It can be seen that PV inverters must be oversized to comply with the PF requirements even at full active power generation (Curve A, Fig. 2).

Likewise, the recent Italian standard CEI 0–2 [43] states similar operating conditions for DGs connected to LV networks. For units between 3 and 6 kVA, an adjustable PF of $0.95_{leading}$ to $0.95_{lagging}$ is necessary, while for larger units a rectangular capability is required as sketched in Fig. 2 [41].

Finally, while it is technically possible to design PV inverters to provide reactive support at smaller PF values or even if solar input is zero, much like a STATCOM, this functionality is not standard in the industry. The standards dictate the upper and lower bounds on reactive power with respect to active power and rating of the inverter, and manufacturers must comply with these. However, such functionality might be provided by future PV inverters. Thus, in Section V-B the benefits arising from this operation are discussed.

III. Distributed Control Scheme

The proposed controller is implemented at the inverter level, taking as input the locally measured terminal voltage (V_{tm}) and setting the active and reactive power set-points (P_{set}, Q_{set}). Each controller is implemented as a discrete device, updating the control actions with a period T_{upd}, that is the

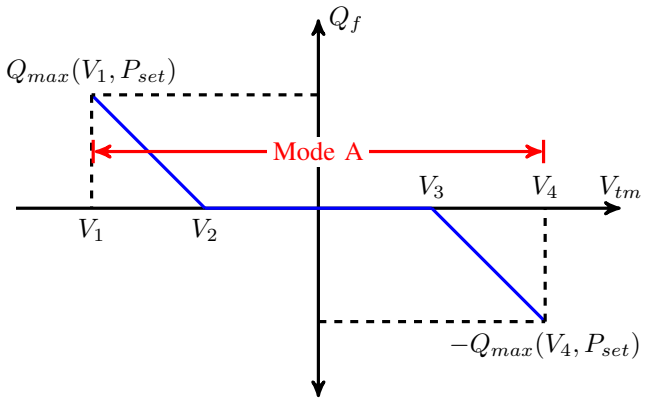

Figure 4. $Q_f(V_{tm}, P_{set})$ function for Mode A. For $V_{tm} \geq V_4$ an emergency signal is issued and the controller moves to Mode B.

n-th action takes place at time $t_n = nT_{upd}$. This discrete nature is due to the use of embedded microcontrollers and the communication, measuring and computing delays involved in the procedure.

As summarized in the Introduction, the controllers have five modes of operation. They are shown in Fig. 3, and detailed in the remaining of this section.

A. Mode A: Normal operating conditions

During normal operating conditions, when all PV terminal voltages in the LV feeder are below a predefined maximum V_4, the PV units follow an MPPT logic for active power set-point and adjust the reactive power as a function of their terminal voltage, as shown in Fig. 4, inspired of Ref. [44], and firstly introduced in [15]. The reactive power adjustment is aimed at counteracting overvoltages when V_{tm} exceeds V_3. The symmetrical part of the reference figure is used in undervoltage situations, which are not considered in this study.

In this mode of operation only local measurements are used and no communication among the controllers is needed.

B. Mode B: Coordinated reactive power adjustment

A PV unit whose terminal voltage has reached V_4, has already made full use of its reactive power adjustment capability and cannot mitigate the overvoltage by itself without proceeding to active power curtailment. At this moment and for as long as the overvoltage persists, a repeating distress signal is sent to all PV controllers in the same feeder as sketched in Fig. 5.

Upon receiving this signal, all PV controllers in the same feeder start adjusting their reactive power consumptions to decrease the terminal voltage of the distressed PV(s). During this mode of operation, the PV units follow an MPPT logic for active power set-point while increasingly consuming more reactive power with the target of reaching their $-Q_{max}$ values at $t = t_{DQ}$. More specifically, Q_{set} is adjusted as follows:

$$Q_{set}[t_n] = Q_{set}[t_{n-1}] + (-Q_{max}[t_n] - Q_{set}[t_{n-1}]) \frac{t_n - t_{n-1}}{t_{DQ} - t_{n-1}} \quad (2)$$

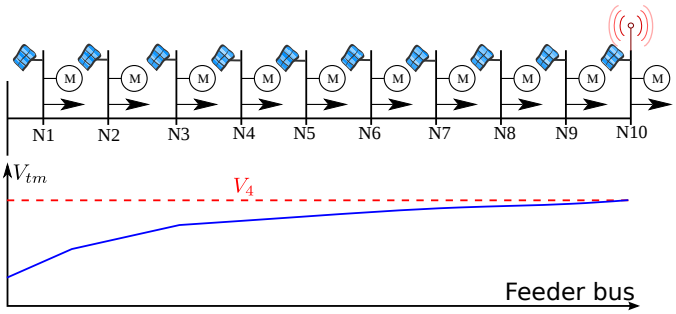

Figure 5. Feeder emergency signal

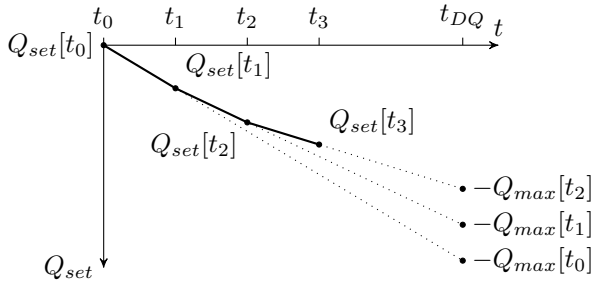

Figure 6. Mode B: Q_{set} adjustment

where the value of $Q_{max}[t_n] = Q_{max}(V_{tm}[t_n], P_{set}[t_n])$ is updated at each step based on the capability curve (Fig. 2) and t_{DQ} is calculated based on the first distress signal received. An example of this adjustment is presented in Fig. 6.

This mode of operation has two possible outcomes. If the overvoltage problem persists after t_{DQ}, the PV controllers proceed to coordinated active power curtailment (Mode C) while having reached $Q_{set} = -Q_{max}$. On the other hand, if the problem has been resolved only with the use of reactive power adjustments, the PV controllers freeze their reactive power set-points while continuing to follow the MPPT logic for active power. After a time T_{reset} without new distress signals, the PV units move to Mode E, where they try to restore Q_{set} to the value given in Fig. 4 for normal operating conditions (Mode A).

C. Mode C: Active power curtailment

In this mode, the PV controllers stop applying MPPT and start curtailing active power according to:

$$P_{set}[t_n] = P_{out}[t_0] \left(1 - \frac{t_n - t_{n-1}}{t_{DP} - t_{n-1}}\right) \quad (3)$$

where $P_{out}[t_0]$ is the PV unit's active power output at the moment t_0 of entering Mode C and t_{DP} is the time by which all PV units need to have curtailed all their active power outputs, calculated based on the time of entering Mode C.

In this mode, the reactive power set-point keeps being adjusted to $-Q_{max}(V_{tm}[t_n], P_{set}[t_n])$, with the latter being updated due to the variations of the active power and the change of terminal voltage, as dictated by the capability curve. That is, for the capability curve sketched in Fig. 2, Q_{max} will reach zero at t_{DP} as the active power reaches zero.

If the overvoltage problem is resolved, that is no more emergency signals are received, the PV controllers freeze their power set-points and timers. Then, after a period of T_{reset} without new distress signals, the controllers move to Mode D.

However, if the PV units in the distressed feeder have exhausted all their possible controls and the overvoltage problem persists, then the problem was not created by the PV generation. At the end of Mode C, the active power output of all PV units is at zero. Any overvoltages in such passive feeders is a consequence of MV voltages or MV/LV transformer set-points. In such a particular case, the controllers remain in Mode C so as not to further aggravate the problem.

D. Mode D: Restoring active power generation

The PV controllers reach this mode after having curtailed active power generation (Mode C) and not receiving a distress signal over a period T_{reset}. The purpose of this mode is to smoothly and uniformly restore the active power generation of the PV units to the MPP values, without creating new overvoltage problems. Thus, the active power set-point is modified as:

$$P_{set}[t_n] = P_{max}\frac{t_n - t_{n-1}}{t_{RP} - t_{n-1}} \tag{4}$$

where P_{max} is the PV unit's nominal active power output and t_{RP} is the time by which all PV units need to have restored to their MPP value, calculated based on the time of entering Mode D.

During this active power restoration mode, the reactive power set-point is fixed to $-Q_{max}(V_{tm}[t_n], P_{set}[t_n])$, with the latter being updated due to the variations of the active power and the change of terminal voltage, as dictated by the capability curve (Fig. 2).

If the problem reoccurs (a new distress signal is received) during the active power increase, the PV units move back to Mode C. Otherwise, at time $t = t_{RP}$, all the PV units have reached $P_{set} = P_{max}$, hence MPP output, and they move to Mode E.

E. Mode E: Restoring reactive power to Mode A set-point

The PV units in a feeder reach this mode either from Mode D or directly from Mode B after T_{reset} time without a distress signal. The purpose of this mode is to smoothly adjust the reactive power set-points Q_{set} of the PV units according to Fig. 4 while keeping active power output to MPP values. The reactive power set-point is modified as:

$$\begin{aligned} Q_{set}[t_n] = Q_{set}[t_{n-1}] \\ + (Q_f[t_n] - Q_{set}[t_{n-1}])\,\frac{t_n - t_{n-1}}{t_{RQ} - t_{n-1}} \end{aligned} \tag{5}$$

where the value of $Q_f[t_n] = Q_f(V_{tm}[t_n], P_{MPP}[t_n])$ and t_{RQ} is the time by which all PV units need to have restored their reactive powers, calculated based on the time of entering Mode E.

If an overvoltage problem re-occurs (a new distress signal is received) during the reactive power restoration, the PV units move back to Mode B. Otherwise, at time $t = t_{RQ}$, all the PV units have reached $Q_{set} = Q_f(V_{tm}, P_{MPP})$ and, hence, they have come back to Mode A.

F. General considerations

The proposed distributed scheme makes no use of the network model or parameters. Moreover, it does not need information on the position of each PV inside the LV feeder. In normal operating conditions (Mode A), there is no exchange of information among the controllers. Limited communication, in the form of a distress signal, is needed for Modes B and C.

The proposed scheme is designed so that at the end of Mode C all PV units in the distressed feeder will have curtailed the same percentage of their active power at normal operating conditions ($P_{out}[t_0]$). In this way, the financial loss from curtailing active power is shared evenly amongst all the PV units. In reality though, as will be shown in Section V, some minor differences between them exist due to communication delays and the discrete and asynchronous nature of embedded controllers.

In this work it is assumed that the voltages without the PV injections (only loads) are within the acceptable limits. If this assumption does not hold, it is possible to meet situations where in the same LV feeder exist both buses with over- and under-voltage conditions. If this scenario occurs, the units with undervoltage problems will not contribute to the coordinated reduction but will remain in Mode A, that is producing P_{MPP} and adjusting their reactive power according to Fig. 4. Such cases, however, are not considered in this study.

IV. Performance evaluation

To assess its performance, the proposed scheme is compared to a centralized one whose objective is to minimize the active power curtailment while satisfying the network voltage constraints. This type of optimization problem belongs to the general class of OPF problems.

A. Optimal Power Flow formulation and solution

Let $\mathcal{B}$ be the set of buses of the network. Each bus is characterized by the magnitude V and the phase angle θ of its voltage. Let $\mathcal{PV}$ be the subset of buses of $\mathcal{B}$ to which PV units are connected. A PV unit is characterized by five elements: P_{PV}, the active power supplied by the inverter to the grid, Q_{PV}, the reactive power supplied to the grid, P_{PV}^{MPP}, the maximum active power the PV panels can produce given the current sunlight and temperature, $I_{PV}^{\max}$, the maximum current of the inverter, and $PF_{PV}^{\min}$, the minimal power factor under which the inverter can operate.

The minimization of the total curtailed active power in the whole network is taken as objective:

$$\min_{P_{PV}, Q_{PV}, V, \theta} \quad \sum_{j \in \mathcal{PV}} P_{PV_j}^{MPP} - P_{PV_j} \tag{6}$$

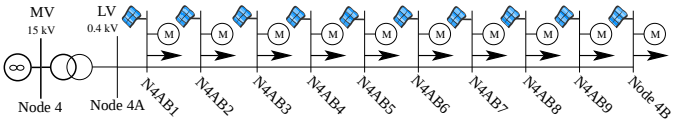

Figure 7. Single feeder model

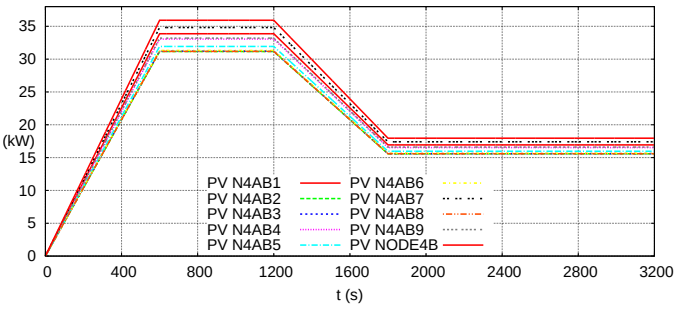

Figure 8. Single feeder input power (P_{MPP})

subject to

$$h(P_{PV}, Q_{PV}, P_{inj}, Q_{inj}, V, \theta) = 0 \quad (7)$$

$$V^{\min} \leq V_j \leq V^{\max}, \quad j \in \mathcal{PV} \quad (8)$$

$$0 \leq P_{PV_j} \leq P_{PV_j}^{MPP}, \quad j \in \mathcal{PV} \quad (9)$$

$$\sqrt{(P_{PV_j})^2 + (Q_{PV_j})^2} \leq I_{PV_j}^{\max} \cdot V_j, \quad j \in \mathcal{PV} \quad (10)$$

$$\frac{P_{PV_j}}{\sqrt{(P_{PV_j})^2 + (Q_{PV_j})^2}} \geq PF_{PV_j}^{\min}, \quad j \in \mathcal{PV} \quad (11)$$

- equation (7) is a compact notation for the power flow equations, P_{inj} (resp. Q_{inj}) is a vector of active (resp. reactive) powers injected at each bus by other equipment than the PV installations (loads are considered to inject negative power);
- inequality (8) forces voltages to stay within their limits;
- inequality (9) stresses that the active power injected by the inverter should be positive and no larger than the maximal power that the PV panel can produce;
- inequality (10) sets a limit on the current the inverter can supply;
- inequality (11) puts a limit on the power factor.

It should be noted that the constraints defined here are the same as the one directly or indirectly implemented in the distributed scheme. The problem is solved with MATLAB optimization toolbox, using interior point method.

B. Comparison with a centralized scheme

To assess the performance of the distributed scheme, the following procedure was used.

A step change from zero to a chosen value is applied to P_{MPP}, aiming to cause overvoltage problems. The response of the system with the use of distributed controllers is simulated until an equilibrium point is reached. The total amount of active power produced or curtailed and the reactive power absorbed by the PV units are then extracted.

Similarly, the system's response to the same step change of P_{MPP} is simulated when the OPF problem (6)–(11) is solved

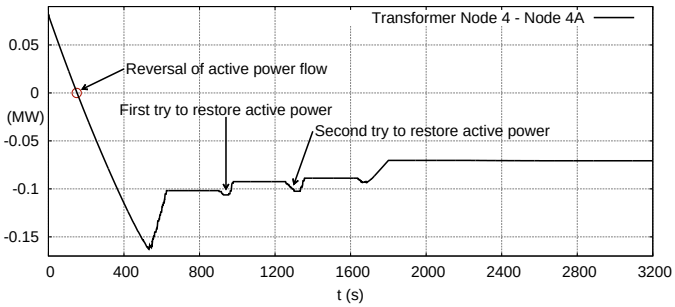

Figure 9. Active power flow in the MV/LV transformer of the feeder (negative values mean exportation of power to the MV level)

to acquire the PV units' set-points. The corresponding values of the total active power produced or curtailed, the reactive power absorbed by the PV units and the network losses are used to evaluate the performance of the distributed scheme.

V. Simulation Results

The performance of the proposed scheme has been tested using dynamic simulations, first on a single LV feeder, then on a larger MV/LV network including 14 LV feeders. The simulations, in phasor mode, have been performed using the RAMSES [45] software developed at the University of Liège.

A. Single feeder example

The single LV feeder in Fig. 7 is used to further illustrate the various modes of operation and the behavior of the distributed controllers. Each bus includes a PV unit, an equivalent motor and a voltage dependent load. For the sake of simplicity the same fraction of motor load is considered for all loads, namely 30%. Each equivalent induction motor has a 6-kVA rated apparent power and its model accounts for the presence of a double-cage rotor.

The lines have a X/R ratio of 0.89. The X/R ratio dictates how much the voltages are affected by active power or reactive power changes. If the X/R ratio is high, then reactive power dominates the voltage changes. On the other hand, distribution networks typically have a low X/R ratio. Hence, reactive support may not be sufficient to control voltages and active power changes are needed [46]. However, the distributed algorithm controls first the reactive power as it is considered to be a cheap resource from the producer point of view, and then active power. The outcome does not depend on the X/R ratio but it affects how much active power will be curtailed to prevent overvoltages, if any.

The nominal power of each PV unit was randomly selected between 30.5 and 37.5 kW. The model follows the capability curve in Fig. 2 and is equipped with the proposed controller with the activation period T_{upd} randomly drawn between 22 and 30 seconds. Finally, the control parameters were chosen at $V_4 = 1.07$ pu, $V_3 = 1.02$ pu, $PF_{min} = 0.95$, $T_{DQ} = 300$ s, $T_{DP} = 300$ s, $T_{RP} = 600$ s, $T_{RQ} = 600$ s and $T_{reset} = 300$ s.

The smooth solar power (P_{MPP}) variation in Fig. 8 is considered over a period of 3200 s. P_{MPP} starts from zero and reaches a randomly chosen value between 90 and 100%

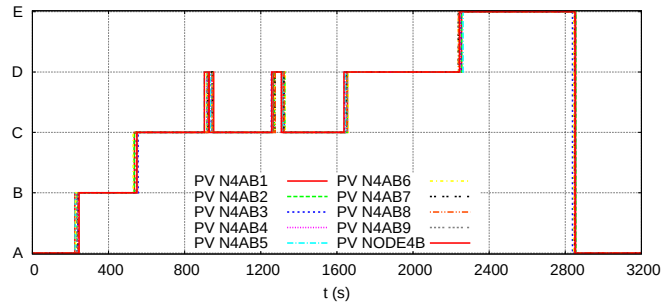

Figure 10. Single feeder state transitions

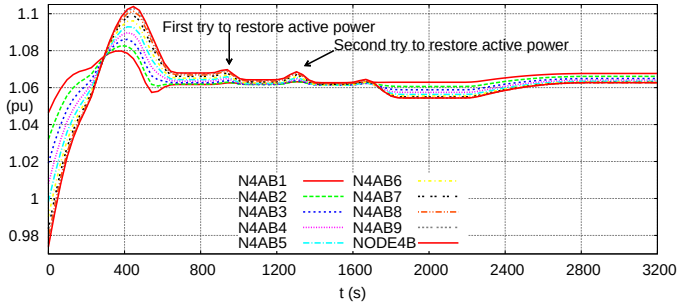

Figure 11. Single feeder voltages

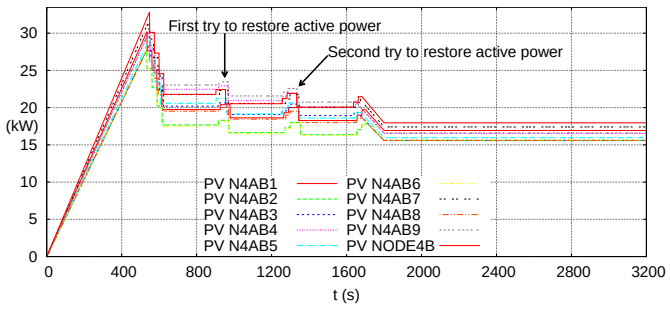

Figure 12. Single feeder PV active power

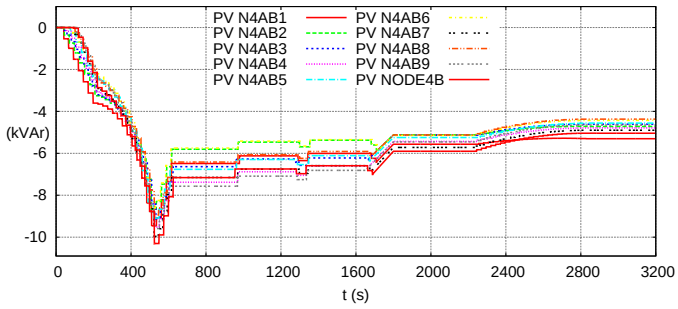

Figure 13. Single feeder PV reactive power

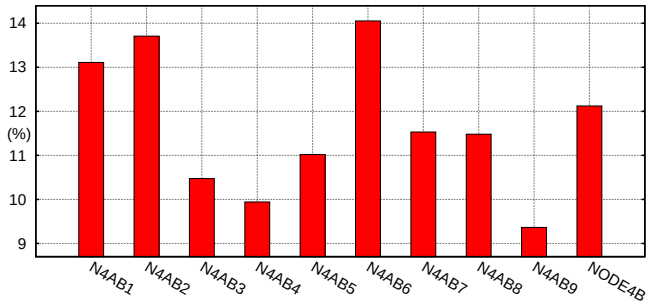

Figure 14. Single feeder energy lost by every PV ($T_{upd} = 22 \sim 30$ s)

of the PV unit's nominal power after 600 s. From 1200 s on, P_{MPP} smoothly decreases to reach 50% of its maximal value. The loads vary only with their voltages during this period of time.

Initially, all PV units are at zero generation and the LV feeder is importing its whole active power from the MV system. Moreover, as all terminal voltages are lower than V_4, the distributed controllers are in Mode A.

As PV generation increases, due to the increase of P_{MPP}, the imported active power decreases at the profit of locally generated one. This can be seen in Fig. 9, depicting the active power transfer through the transformer. From the same figure, it can be seen that at $t \approx 200$ s, the LV feeder starts exporting active power to the MV network.

Figures 10 to 13 show the various state transitions of the controllers, the voltages at the connection points of the PV units, the active and reactive power output of the inverters, respectively.

Along with the PV active power increase, the LV bus voltages rise and the reactive power is adjusted according to Fig. 4. This leads, in turn, to a smooth increase of the reactive power absorption by the inverters as seen in Fig.13.

At $t \approx 250$ s, an overvoltage takes place and a distress signal is sent by PV unit *N4AB1* (see Fig. 7) through the feeder. Consequently, all controllers move to Mode B and gradually absorb more reactive power targeting to reach their maximum after $T_{DQ} = 300$ s, i.e. $t = t_{DQ} \approx 550$ s.

Since the attempt to deal with the overvoltage by means of reactive power adjustments fails, the controllers go to Mode C and start curtailing active power at $t \approx 550$ s. As can be seen in Fig. 12, active power is curtailed until all voltages decrease under $V_4 = 1.07$ pu at $t \approx 600$ s.

Following, after a period T_{reset} with no other overvoltage alarm, at $t \approx 900$ s the controllers enter the restoration phase and try to increase the active power production (Mode D). However, this increase results in overvoltage and the controllers move back to Mode C. This attempt is reiterated after a second T_{reset} period, at $t \approx 1250$ s, with the same result.

The smooth decrease of P_{MPP} after $t = 1200$ s limits the active power production. Thus, during the third attempt in Mode D, at $t \approx 1620$ s, active power restoration to P_{MPP} is successful.

In the last part of simulation, the controllers move to Mode E and slowly decrease their reactive power absorption. Once reaching the values dictated by the curve in Fig. 4, the controllers proceed to Mode A and the system returns to its final state.

Figure 14 shows the percentage of electrical energy lost by each PV unit due to curtailment, computed as:

$$Energy\ Lost_{PV_j} = \frac{\int_0^{3200} P_{PV_j}^{MPP} dt - \int_0^{3200} P_{PV_j}^{out} dt}{\int_0^{3200} P_{PV_j}^{MPP} dt} \quad (12)$$

Table I
COMPARISON BETWEEN ACTIVE AND REACTIVE POWER GENERATED AND CURTAILED BY PV UNITS AND NETWORK LOSSES WITH THE DISTRIBUTED AND CENTRALIZED SCHEME FOR THE TWO TEST-SYSTEMS

	Single feeder		14-feeder	
	Dist.	Centr.	Dist.	Centr.
Active power generated (kW)	204	249	1460	1475
Active power curtailed (kW)	123	78	18.4	0
Reactive power absorbed (kVar)	67.1	81.8	367	365
Losses in the network (kW)	20.5	27.3	123	125

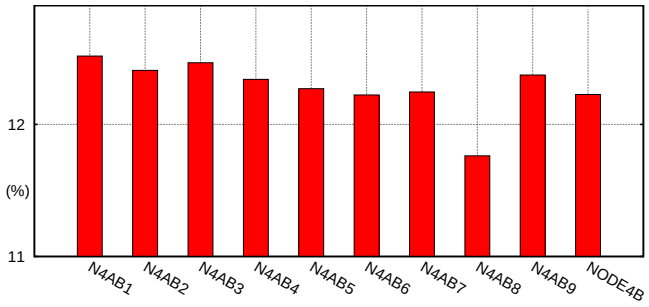

Figure 15. Single feeder energy lost by every PV ($T_{upd} = 1$ s)

It can be seen that all PV units have similar values, with the variations between them caused by the asynchronous and discrete nature of the controllers. To verify this behavior, the simulation is repeated with $T_{upd} = 1$ s and $T_{upd} = 0$ s respectively.

In the first case, it is assumed that the measurement, control and communication delays are 1 s and the energy lost is seen in Fig. 15. It can be seen that the variation between the different PV units has been significantly decreased. In the second case, it is assumed that the controllers are infinitely fast without any measurement or communication delays. The energy lost in this case is the same for all PV units and equal to 12.2%.

The performance of the proposed control is compared to that of an OPF-based centralized scheme, as explained in Section IV-B. A step change of P_{MPP} is applied causing an overvoltage problem. Figure 16 displays the active power output by the PV units for both the distributed and the

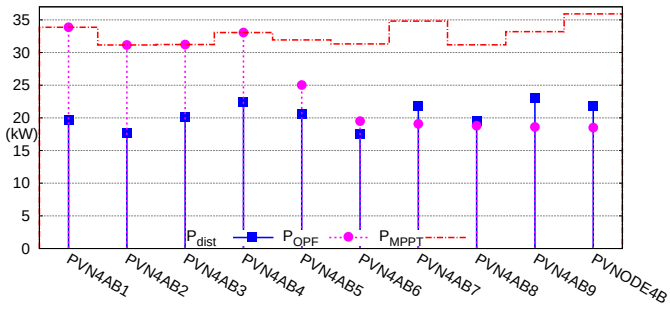

Figure 16. Active power production by each PV unit, with squares for the distributed and circles for the centralized scheme, at the end of Mode C. The maximum power that could be produced by each PV unit is shown by the upper dash-dotted line. The PV units closest to the distribution transformer are on the left

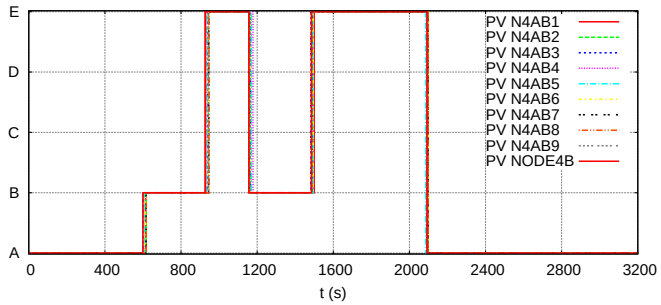

Figure 17. Single feeder state transitions (STATCOM operation)

centralized scheme at their final equilibrium point.

It is observed that the centralized scheme prioritizes curtailing active power of PV units further away from the distribution transformer, where the overvoltage problem is more prominent and the curtailment of active power is more effective. On the other hand, the distributed scheme leads to a more uniformly shared active power curtailment among the PV units.

Table I shows the total active power production and curtailment, the total reactive power absorption and the network losses in the feeder at the equilibrium points. As expected, the distributed scheme curtails more active power than the centralized, 37.6% versus 24.0%. This is the cost associated with uniformly sharing the active power curtailment throughout the feeder and not prioritizing the curtailment on the problematic buses. Moreover, based on the capability curve (see Fig. 2), a higher active power output allows for more reactive power to be absorbed. Thus, the OPF-based approach allows for less active power curtailment and at the same time higher reactive power absorption. Nevertheless, the network losses are higher for this approach because of the larger amount of active and reactive power transiting through the network.

This better performance of the OPF-based scheme is anticipated as the latter can perform a centralized optimization, knowing both the system model and the remote measurements from all the nodes and inverters. As mentioned in the Introduction, the main advantage of the proposed scheme is that it provides a slightly suboptimal solution with far less information and communication requirements.

B. *Selection of the capability curve*

As discussed in Section II the capability curve of Fig. 2 is used in the PV model to calculate the available reactive power. This is implemented through Eq. 1. However, it is technically possible for a PV inverter to operate as a STATCOM device. In this case, the capability curve is defined by the entire semi-circular area of Fig. 2 and can be implemented by redefining Eq. 1 as:

$$I_{qmax} = \sqrt{I_{max}^2 - I_{pcmd}^2} \tag{13}$$

Comparing the two capability curves, it can be clearly seen that PV units operating as STATCOM devices offer higher flexibility in adjusting reactive power, especially when the amount of active power produced is small. Figure 17 shows the state transition of the single feeder example using the STATCOM capability curve. In this case, the controllers never

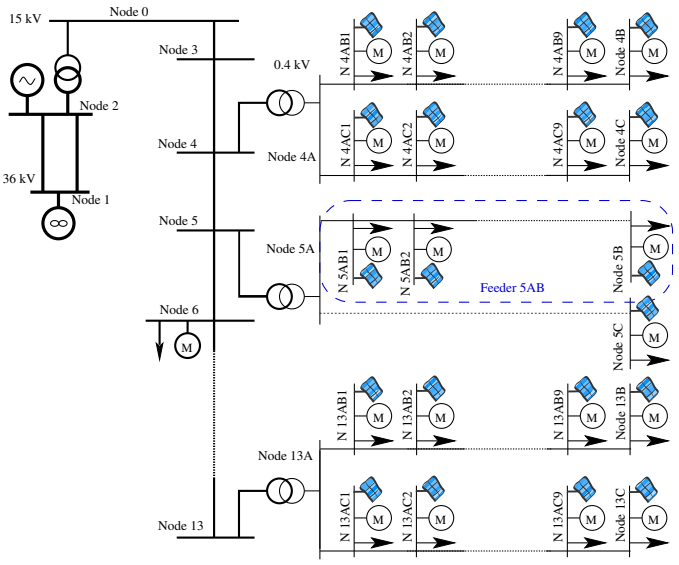

Figure 18. 14-feeder test-system model

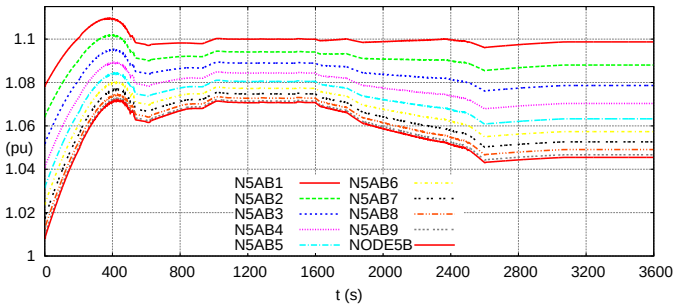

Figure 19. 14-feeder test-system: voltage evolution for feeder 5AB

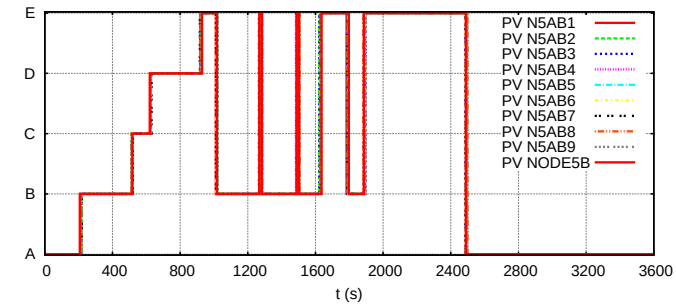

Figure 20. 14-feeder test-system: state transitions for feeder 5AB

reach Mode C and do not curtail any active power; the reactive power adjustments are enough to secure the system.

The proposed control scheme does not make any assumptions on the form of the capability curve; whether this is a more restricted curve like Fig. 2 due to the grid code requirements, a more permissive STATCOM-type or even a combination of the two in the same LV feeder. The scheme uses first the available reactive power control and then proceeds to active power curtailment, if needed.

C. 14-feeder test-system

In this subsection, the MV/LV distribution system presented in [47] is used, modified for the purpose of demonstrating the performance of the method in a demanding situation. Its one-line diagram is shown partially in Fig. 18. The system includes 14 LV feeders similar to the one considered in the previous subsection. The feeders are connected in pairs to the MV buses 4, 5, 7, 8, 10, 11 and 13. Larger motors are connected to the MV buses 6, 9 and 12. Furthermore, a synchronous machine with detailed model is connected to Node 2.

The same variation of P_{MPP}, as in the previous system, is considered for each feeder. The nominal power of the PV units in this case was randomly chosen between 9.5 and 12.5 kW. The control parameters were chosen at $V_4 = 1.10$ pu, $V_3 = 1.05$ pu, $PF_{min} = 0.95$, $T_{DQ} = 300$ s, $T_{DP} = 600$ s, $T_{RP} = 600$ s, $T_{RQ} = 300$ s and $T_{reset} = 100$ s.

From Fig. 19, it can be observed that the distributed scheme successfully manages to keep voltages below 1.1 p.u. after a temporary excess that starts at $t = 200$ s. The controller state transitions are presented in Fig. 20. It can be seen that controllers switch to Mode B when an overvoltage takes place at $t \approx 200$ s. As reactive power support is not sufficient to clear the overvoltage situation, they proceed to Mode C and start curtailing active power. Controllers then enter the restorative phase of the algorithm until they reach Mode E where an overvoltage occurs. Next, they switch back and forth between Mode B and E. At $t \approx 2500$ s, the controllers manage to reach the normal mode of operation (Mode A) without creating an overvoltage situation.

Table II shows the total active power curtailment (as a percentage of P_{MPP}) and the reactive power absorbed (as a percentage of Q_{max}) for each feeder at the end of Mode C ($t \approx 620$ s). It can be seen that LV feeders located closer to the HV/MV transformer have to curtail some active power while the more remote ones rely only on reactive power adjustments. This is expected as the voltage at the MV buses further from the HV/MV transformer are lower and, hence, the voltage rise along the LV feeder does not result in excessive voltages. Moreover, there is no communication between the feeders, thus the control actions rely only on local measurements within each feeder.

Finally, Table I shows the total active power production and curtailment, the total reactive power absorption and the network losses in the feeder at the equilibrium points after a

Table II
PERCENTAGE OF CURTAILED ACTIVE POWER (P_{curt}) AND ABSORPTION OF REACTIVE POWER (Q_{abs}) IN PERCENTAGE OF THE TOTAL POWER PER FEEDER AT THE END OF MODE C ($t \approx 620$ S).

Feeder	P_{curt}	Q_{abs}	Feeder	P_{curt}	Q_{abs}
4AB	1.89%	100.0%	8AC	0.00%	65.7%
4AC	2.76%	100.0%	10AB	0.00%	67.2%
5AB	5.61%	100.0%	10AC	0.00%	64.4%
5AC	6.78%	100.0%	11AB	0.00%	59.2%
7AB	0.37%	100.0%	11AC	0.00%	60.5%
7AC	0.00%	100.0%	13AB	0.00%	75.5%
8AB	0.00%	65.2%	13AC	0.00%	78.1%

step change of P_{MPP}. It can be seen that the proposed scheme performs almost as well as the OPF-based one and that the system losses are almost equal in both schemes. Nevertheless, the former resorts to some active power curtailment whereas the latter utilizes only reactive power adjustments to resolve the overvoltage problem. This is to be expected as the OPF-based controller optimizes the entire MV/LV network and can provide support between separate feeders. On the contrary, the distributed scheme coordinates only PV units within the same feeder and does not know about the other LV feeders.

VI. Conclusion

As an alternative to network reinforcement, a distributed control scheme that alleviates the voltage problems caused by a large penetration of PV units in LV DNs has been proposed. This scheme makes use of little communication between the controllers to activate the inverters' reactive support and minimize active power curtailment. Through dynamic simulations, the behavior of the scheme has been analyzed and it was shown that its performance is comparable to a centralized, OPF-based, control scheme which would be more expensive to deploy and complex to operate (for instance, when the DN topology changes).

Several research directions exist for this distributed control scheme. First, it would be interesting to extend it to an unbalanced three-phase network. Unbalances can be generally neglected in MV networks in Europe but unbalances are often present in LV DNs since house appliances and PV units are usually single phase. This implies taking into account the coupling between the phases.

Second, rather than relying on active power curtailment, the use of local storage systems or flexible loads could be considered. This would change fundamentally the control problem considered and would raise new research questions. For example, the existence of local energy storage would couple the control actions at different times, since accumulating active power into storage at a specific time, influences the amount of energy available in the future.

Finally, a cost analysis could be performed to evaluate the economical profitability of deploying such a distributed scheme compared to a reinforcement of the network.

Acknowledgment

The financial support of this research by the Walloon region in the framework of the PREMASOL project (Ref. C-6829) is gratefully acknowledged. Maria-Emilia Hervas from GreenWatch is also thanked for coordinating that project.

References

[1] P. Maycock, "The future of energy summit 2013. Bloomberg New Energy Finance." Available: htt://bnef.com/Presentations/download/136 [Accessed January 2014].

[2] M. Bazilian, I. Onyeji, M. Liebreich, I. MacGill, J. Chase, J. Shah, D. Gielen, D. Arent, D. Landfear, and S. Zhengrong, "Re-considering the economics of photovoltaic power," *Renewable Energy*, vol. 53, pp. 329–338, May 2013.

[3] R. Schleicher-Tappeser, "How renewables will change electricity markets in the next five years," *Energy Policy*, vol. 48, pp. 64–75, 2012.

[4] C. Masters, "Voltage rise: the big issue when connecting embedded generation to long 11 kV overhead lines," *Power Engineering Journal*, vol. 16, no. 1, pp. 5–12, 2002.

[5] C. Schwaegerl, M. Bollen, K. Karoui, and A. Yagmur, "Voltage control in distribution systems as a limitation of the hosting capacity for distributed energy resources," in *Proc. of CIRED 2005 18th International Conference and Exhibition on Electricity Distribution*, 2005.

[6] P. Barker and R. D. Mello, "Determining the impact of distributed generation on power systems. I. Radial distribution systems," in *Proc. of IEEE PES 2000 Summer Meeting*, vol. 3, pp. 1645–1656, 2000.

[7] J. P. Lopes, N. Hatziargyriou, J. Mutale, P. Djapic, and N. Jenkins, "Integrating distributed generation into electric power systems: A review of drivers, challenges and opportunities," *Electric Power Systems Research*, vol. 77, pp. 1189–1203, July 2007.

[8] S. Liew and G. Strbac, "Maximising penetration of wind generation in existing distribution networks," *IEE Proceedings – Generation, Transmission and Distribution*, vol. 149, no. 3, pp. 256–262, 2002.

[9] A. Bonfiglio, M. Brignone, F. Delfino, and R. Procopio, "Optimal control and operation of grid-connected photovoltaic production units for voltage support in medium-voltage networks," *IEEE Transactions on Sustainable Energy*, vol. 5, pp. 254–263, Jan. 2014.

[10] Y. P. Agalgaonkar, B. C. Pal, and R. A. Jabr, "Distribution voltage control considering the impact of PV generation on tap changers and autonomous regulators," *IEEE Transactions on Power Systems*, vol. 29, pp. 182–192, Jan. 2014.

[11] M. Farivar, R. Neal, C. Clarke, and S. Low, "Optimal inverter VAR control in distribution systems with high PV penetration," in *Proc. of IEEE PES 2012 General Meeting*, July 2012.

[12] L. F. Ochoa and G. P. Harrison, "Minimizing Energy Losses: Optimal Accommodation and Smart Operation of Renewable Distributed Generation," *IEEE Transactions on Power Systems*, vol. 26, pp. 198–205, Feb. 2011.

[13] H.-G. Yeh, D. F. Gayme, and S. H. Low, "Adaptive VAR control for distribution circuits with photovoltaic generators," *IEEE Transactions on Power Systems*, vol. 27, pp. 1656–1663, Aug. 2012.

[14] Q. Gemine, E. Karangelos, D. Ernst, and B. Cornelusse, "Active network management: Planning under uncertainty for exploiting load modulation," in *Proc. of IREP 2013 Symposium on Bulk Power System Dynamics and Control - IX Optimization, Security and Control of the Emerging Power Grid*, 2013.

[15] M. Bollen and A. Sannino, "Voltage control with inverter-based distributed generation," *IEEE Transactions on Power Delivery*, vol. 20, no. 1, pp. 519–520, 2005.

[16] K. Turitsyn, P. Sulc, S. Backhaus, and M. Chertkov, "Options for Control of Reactive Power by Distributed Photovoltaic Generators," *Proceedings of the IEEE*, vol. 99, pp. 1063–1073, June 2011.

[17] E. Demirok, P. C. González, K. H. B. Frederiksen, D. Sera, P. Rodriguez, and R. Teodorescu, "Local reactive power control methods for overvoltage prevention of distributed solar inverters in low-voltage grids," *IEEE Journal of Photovoltaics*, vol. 1, pp. 174–182, Oct. 2011.

[18] M. García-Gracia, N. El Halabi, H. Ajami, and M. P. Comech, "Integrated control technique for compliance of solar photovoltaic installation grid codes," *IEEE Transactions on Energy Conversion*, vol. 27, pp. 792–798, Sept. 2012.

[19] R. Tonkoski, L. A. C. Lopes, and T. H. M. El-Fouly, "Coordinated active power curtailment of grid connected PV inverters for overvoltage prevention," *IEEE Transactions on Sustainable Energy*, vol. 2, pp. 139–147, Apr. 2011.

[20] M. J. E. Alam, K. M. Muttaqi, and D. Sutanto, "Mitigation of rooftop solar PV impacts and evening peak support by managing available capacity of distributed energy storage systems," *IEEE Transactions on Power Systems*, vol. 28, pp. 3874–3884, Nov. 2013.

[21] P. Carvalho, P. Correia, and L. Ferreira, "Distributed reactive power generation control for voltage rise mitigation in distribution networks," *IEEE Transactions on Power Systems*, vol. 23, pp. 766–772, May 2008.

[22] R. Aghatehrani and A. Golnas, "Reactive power control of photovoltaic systems based on the voltage sensitivity analysis," in *Proc. of IEEE PES 2012 General Meeting*, July 2012.

[23] N. Kakimoto, Q.-Y. Piao, and H. Ito, "Voltage control of photovoltaic generator in combination with series reactor," *IEEE Transactions on Sustainable Energy*, vol. 2, pp. 374–382, Oct. 2011.

[24] H. Xin, Z. Qu, Z. Lu, D. Gan, and D. Qi, "Cooperative control strategy for multiple photovoltaic generators in distribution networks," *IET Control Theory and Applications*, vol. 5, pp. 1617–1629, Sept. 2011.

[25] H. Xin, Z. Qu, J. Seuss, and A. Maknouninejad, "A self-organizing strategy for power flow control of photovoltaic generators in a distribution

network," *IEEE Transactions on Power Systems*, vol. 26, pp. 1462–1473, Aug. 2011.
[26] H. E. Farag, E. F. El-Saadany, and R. Seethapathy, "A two ways communication-based bistributed control for voltage regulation in smart distribution feeders," *IEEE Transactions on Smart Grid*, vol. 3, pp. 271–281, Mar. 2012.
[27] R. K. Varma, V. Khadkikar, and R. Seethapathy, "Nighttime application of PV solar farm as STATCOM to regulate grid voltage," *IEEE Transactions on Energy Conversion*, vol. 24, pp. 983–985, Dec. 2009.
[28] A. Kiprakis and A. Wallace, "Maximising energy capture from distributed generators in weak networks," *IEE Proceedings - Generation, Transmission and Distribution*, vol. 151, no. 5, pp. 611–618, 2004.
[29] P. N. Vovos, A. E. Kiprakis, A. R. Wallace, and G. P. Harrison, "Centralized and distributed voltage control: impact on distributed generation penetration," *IEEE Transactions on Power Systems*, vol. 22, pp. 476–483, Feb. 2007.
[30] A. Samadi, R. Eriksson, L. Soder, B. G. Rawn, and J. C. Boemer, "Coordinated active power-dependent voltage regulation in distribution grids with PV systems," *IEEE Transactions on Power Delivery*, vol. 29, pp. 1454–1464, June 2014.
[31] K. Tanaka, M. Oshiro, S. Toma, A. Yona, T. Senjyu, T. Funabashi, and C.-H. Kim, "Decentralised control of voltage in distribution systems by distributed generators," *IET Generation, Transmission and Distribution*, vol. 4, no. 11, pp. 1251–1260, 2010.
[32] A. Cagnano, E. De Tuglie, M. Liserre, and R. A. Mastromauro, "Online optimal reactive power control strategy of PV inverters," *IEEE Transactions on Industrial Electronics*, vol. 58, pp. 4549–4558, Oct. 2011.
[33] V. Calderaro, G. Conio, V. Galdi, G. Massa, and A. Piccolo, "Optimal decentralized voltage control for distribution systems with inverter-based distributed generators," *IEEE Transactions on Power Systems*, vol. 29, pp. 230–241, Jan. 2014.
[34] A. R. Di Fazio, G. Fusco, and M. Russo, "Decentralized control of distributed generation for voltage profile optimization in smart feeders," *IEEE Transactions on Smart Grid*, vol. 4, pp. 1586–1596, Sept. 2013.
[35] C. Ahn and H. Peng, "Decentralized voltage control to minimize distribution power loss of microgrids," *IEEE Transactions on Smart Grid*, vol. 4, pp. 1297–1304, Sept. 2013.
[36] S. Galli, A. Scaglione, and Z. Wang, "Power line communications and the smart grid," in *Proc. of IEEE 2010 First International Conference on Smart Grid Communications*, pp. 303–308, Oct. 2010.
[37] X. Carcelle, *Power Line Communications in Practice*. Artech House Telecommunications Library, Artech House, Incorporated, 2009.
[38] WECC REMTF, "Generic solar photovoltaic system dynamic simulation model specification," Sept. 2012. Available: http://www.wecc.biz/ [Accessed January 2014].
[39] R. Caldon, M. Coppo, and R. Turri, "Coordinated voltage control in MV and LV distribution networks with inverter-interfaced users," in *Proc. of IEEE PES 2013 Grenoble PowerTech Conference*, June 2013.
[40] P. Kotsampopoulos, N. Hatziargyriou, B. Bletterie, and G. Lauss, "Review, analysis and recommendations on recent guidelines for the provision of ancillary services by distributed Generation," in *Proc. of IEEE 2013 International Workshop on Inteligent Energy Systems (IWIES)*, pp. 185–190, Nov. 2013.
[41] R. Caldon, M. Coppo, and R. Turri, "Distributed voltage control strategy for LV networks with inverter-interfaced generators," *Electric Power Systems Research*, vol. 107, pp. 85–92, Feb. 2014.
[42] "VDE-AR-N 4105: Generators connected to the LV distribution network - Technical requirements for the connection to and parallel operation with low-voltage distribution networks," Aug. 2011.
[43] "CEI 0–21: Reference technical rules for connecting active and passive users to networks low-voltage electricity networks of energy providers," Dec. 2011.
[44] R. Dugan, W. Sunderman, and B. Seal, "Advanced inverter controls for distributed resources," in *Proc. of CIRED 2013 22nd International Conference and Exhibition on Electricity Distribution*, pp. 1221–1221, 2013.
[45] P. Aristidou, D. Fabozzi, and T. Van Cutsem, "Dynamic simulation of large-scale power systems using a parallel schur-complement-based decomposition method," *IEEE Transactions on Parallel and Distributed Systems*, vol. 25, pp. 2561–2570, Dec. 2013.
[46] J. Morren, S. W. H. de Haan, and J. A. Ferreira, "Contribution of DG units to voltage control: Active and reactive power limitations," in *Proc. of IEEE PES 2005 Russia PowerTech Conference*, June 2005.
[47] B. Otomega and T. Van Cutsem, "Distributed load interruption and shedding against voltage delayed recovery or instability," in *Proc. of IEEE PES 2013 Grenoble PowerTech Conference*, June 2013.

Frédéric Olivier (S'14) received his M.Sc. degree in electrical engineering from the University of Liège, Belgium, in 2013. He is currently pursuing his Ph.D. at the same university. His research interests are in the control of distributed energy resources connected to distribution networks. In particular, he investigates the problems caused by photovoltaic units connected to low-voltage distribution systems.

Petros Aristidou (S'10) received his Diploma in 2010 from the Department of Electrical and Computer Engineering of the National Technical University of Athens, Greece. He is currently pursuing his Ph.D. in Analysis and Simulation of Power System Dynamics at the Department of Electrical and Computer Engineering of the University of Liège, Belgium. His research interests are in power system dynamics, control and simulation.

Damien Ernst (M'98) received the M.Sc. and Ph.D. degrees in engineering from the University of Liège, Belgium, in 1998 and 2003, respectively. He is currently Full Professor at the University of Liège, where he is affiliated with the Systems and Modeling Research Unit. He is also the holder of the EDF-Luminus Chair on Smart Grids. His research interests include power system control and reinforcement learning.

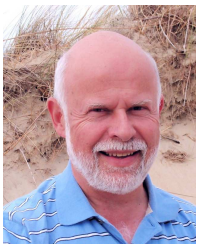

Thierry Van Cutsem (F'05) graduated in Electrical-Mechanical Engineering from the University of Liège, Belgium, where he obtained the Ph.D. degree and he is now teaching electric power systems as adjunct professor. Since 1980, he has been with the Fund for Scientific Research (FNRS), of which he is now a Research Director. His research interests are in power system dynamics, security, monitoring, control and simulation. Part of this research is performed in collaboration with transmission system operators in France, Canada, Greece, Belgium and Germany. He is currently the Past Chair of the IEEE PES Power System Dynamic Performance Committee.